Supplements

LiCSBAS processing implementation

The two most important steps in SBAS-InSAR processing are step 2 (network refinement by loop closure) for removing the low quality interferograms, and step 3 (small baseline network inversion) for inverting the unwrapped phase value into displacement. In steps 2, LiCSBAS checks the reliability of the unwrapped phase interferograms, focusing on removing unwrapping error contaminated interferograms (Morishita et al., 2020). Phase unwrapping errors can occur when the phase difference between adjacent pixels exceeds π radians, leading to inaccuracies in the measured deformation. It groups them in sets of three images at the same pixel values $\Phi 12$, $\Phi 23$, and $\Phi 13$, then using an equation known as the loop phase (also called the closure phase), as shown here:

$$\emptyset_{123} = \emptyset_{12} + \emptyset_{23} - \emptyset_{13} , \tag{S1}$$

When the three interferograms are free from unwrapping errors, the expected loop phase value is approximately zero, although most of the time the values are not exactly zero due to influences such as multi-look, filtering, and changes in soil moisture.

Conversely, if unwrapping errors are present in one or more interferograms, the loop phase tends to align with an integer multiple of 2π. The root mean square (RMS) value of the loop phase image serves as an indicator of the count of pixels affected by unwrapping errors within the loop. Taking the loop phase values of all pixels and calculate the RMS value, if the values exceeds a specific RMS threshold (1.5 radians in our setting) they are flagged as bad quality unwrapping interferogram and are thus excluded from further processing. It is worth noting that the loop phase evaluates unwrapped phase errors for each interferogram, not for each pixel. Based on this reason, during the 20 m resolution SBAS-InSAR processing, we applied a coherence 0.2 mask before the further processing, so the good dry river channel interferograms are not removed due to the high noise in forest areas.

In step 3, LiCSBAS convert the good quality unwrapped phase into displacement. The LiCSBAS software Morishita et al. (2020) uses singular value decomposition (SVD) to solve the phase inversion equation and to get the displacement vector. LiCSBAS software also assumed linear displacement function when crossing the gaps in the network.

The application of the spatial-temporal filter in step 6 was different in 20 m and 100 m resolution processing. For the 100 m resolution, all season data was used as input to remove the residual atmospheric noise while preserving the seasonal sinusoidal non-linear feature of the surface motion time-series. A temporal filter width of 0.15 years (55 days) was set in steps 6. For 20 m resolution processing, no temporal filter was applied in step 6, as only dry season data was used, assuming no residual atmospheric noise.

$$\emptyset_{displacement1} = \frac{4\pi}{\lambda} R_1, \tag{S2}$$

$$\emptyset_{displacement2} = \frac{4\pi}{\lambda} R_2 , \tag{S3}$$

$$\Delta\emptyset_{displacement} = \frac{4\pi}{\lambda} (R_2 - R_1) , \tag{S4}$$

Finally, we converted the line-of-sight (LOS) velocity values to vertical velocity values based on the equation below, which assumes that all observed deformations are vertical.

$$V_{vertical} = \frac{V_{los}}{\cos 38.8°},$$
(S5)

Where 38.8° is the Sentinel-1 satellite SAR acquisition average incident angle (Fig. S3). The incident angle is the angle between the radar beam and the vertical line perpendicular to the Earth surface.
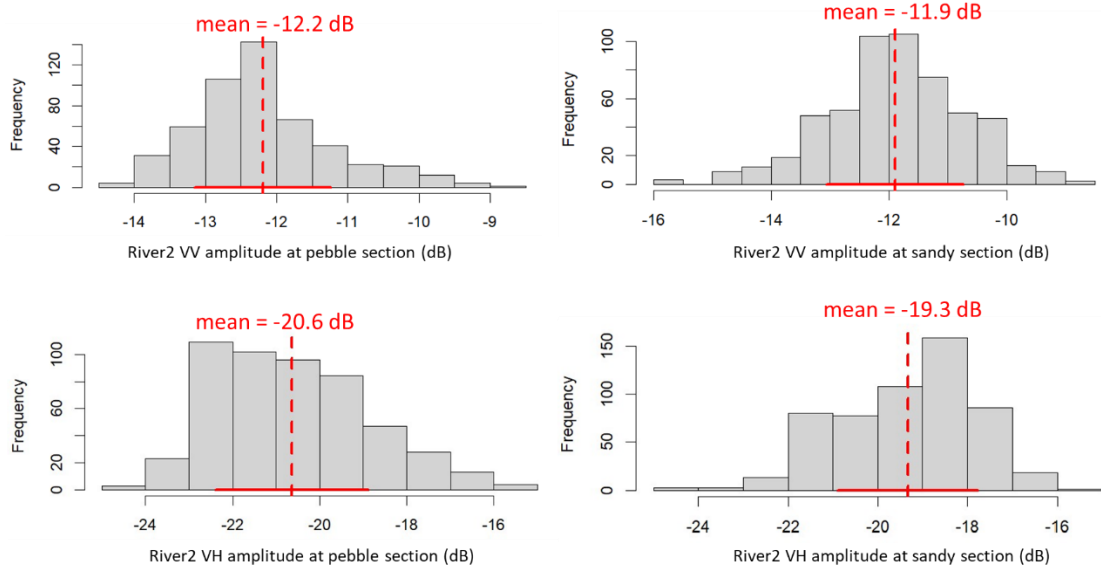

Figure S1: Descriptive statistical analysis of SAR amplitude for the pebble and sandy sections of river 2. The histograms show that the sandy section has a slightly higher mean amplitude compared to the pebble section. The VH amplitude may be more sensitive to differences between pebble and sandy riverbeds due to the slightly larger mean difference. The standard deviations (sd) are similar across all histograms (indicated by red solid lines crossing the mean), with the following values: sd_VV_pebble = 0.9, sd_VV_sandy = 1.1, sd_VH_pebble = 1.7, sd_VH_sandy = 1.5. The standard deviations indicate that the VV amplitude shows less variability from the mean compared to the VH amplitude. The figure was generated in R Studio.
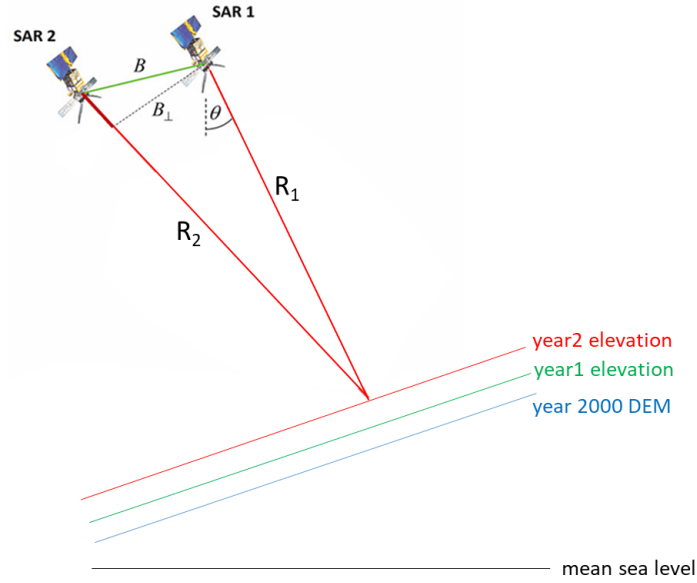
Figure S2: Geometry of satellite SAR acquisition geometry, with parameter of perpendicular bassline (B⊥), incident angle (Ɵ), and distance between satellite and earth surface (R). Modified from Flores-Anderson et al. (2019).
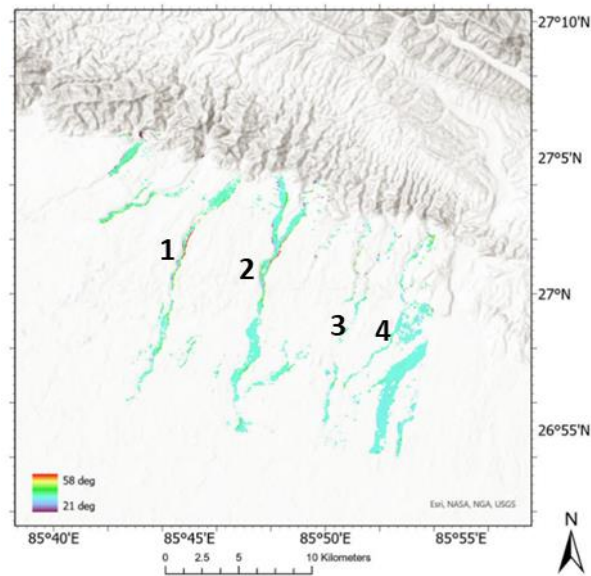
Figure S3: SAR incident angle map acquired on date 29/11/2019, descending frame sourced from the Alaska Satellite Facility (ASF), which illustrates the direction of the radar sensor looking direction. The local incidence angle, measured in degrees, is the angle between the incoming radar beam and the normal to the local surface. The average angle is consistently 38.8° along river channels. This angle is used in Eq. (19) to convert the Line of Sight (LOS) velocity to vertical velocity.
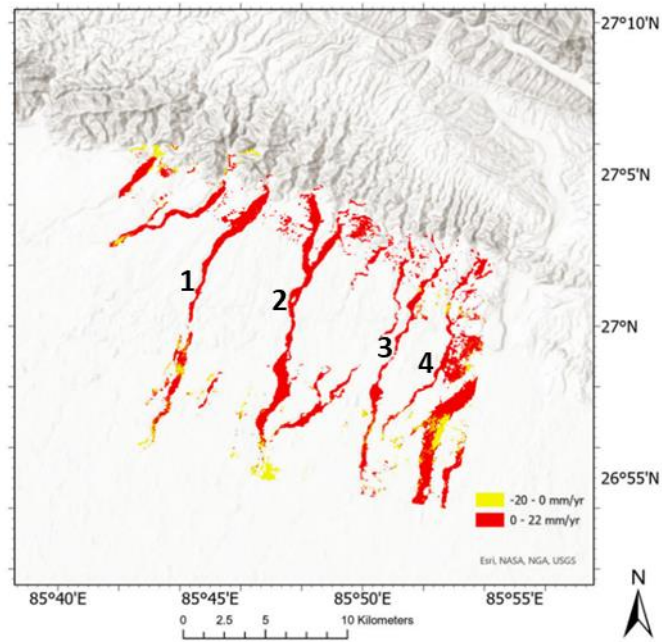
Figure S4: The spatial distribution of riverbed elevation changes from 2016 to 2021. Areas with values above zero are shown in red, indicating areas of sediment deposition. Areas with values below zero are shown in yellow, indicate regions affected by sediment erosion or land subsidence.

65